JOURNAL OF Applied Polymer SCIENCE

Special Issue: Sustainable Polymers and Polymer Science Dedicated to the Life and Work of Richard P. Wool

Guest Editors: Dr Joseph F. Stanzione III (Rowan University, U.S.A.)
and Dr John J. La Scala (U.S. Army Research Laboratory, U.S.A.)

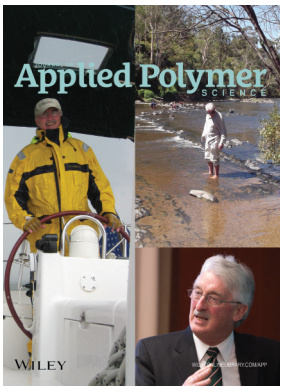

EDITORIAL

REVIEWS

RESEARCH ARTICLES

JOURNAL OF Applied Polymer SCIENCE

Special Issue: Sustainable Polymers and Polymer Science Dedicated to the Life and Work of Richard P. Wool

Guest Editors: Dr Joseph F. Stanzione III (Rowan University, U.S.A.)
and Dr John J. La Scala (U.S. Army Research Laboratory, U.S.A.)

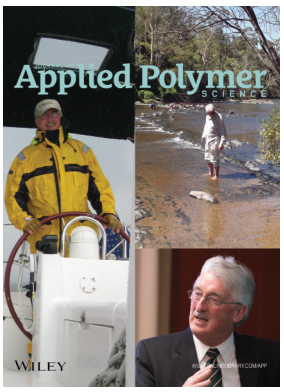

Journal of Applied Polymer Science

Bio-based plasticizer and thermoset polyesters: A green polymer chemistry approach

Mathew D. Rowe,[1] Ersan Eyiler,[2] Keisha B. Walters[1]

[1]Dave C. Swalm School of Chemical Engineering, Mississippi State University, Mississippi State, Mississippi 39762

[2]Department of Chemical Engineering, Cukurova University, Ceyhan, Adana 01950, Turkey

Correspondence to: K. B. Walters (E-mail: kwalters@che.msstate.edu) and E. Eyiler (E-mail: eeyiler@gmail.com)

ABSTRACT: Renewable resource-based polyesters, poly(trimethylene malonate) (PTM) and poly(trimethylene itaconate) (PTI), were synthesized from 1,3-propanediol, malonic acid, and itaconic acid via melt polycondensation using green chemistry principles. Aluminum chloride, a Lewis acid, was used as the catalyst at different reaction temperatures. Chemical structure of PTM and PTI with low dispersities showed the presence of ester and ether bonds. A bimodal molecular weight distribution exists, with the high molecular weight fraction ranging from 22 to 38 kDa while the low molecular weight fraction did not exceed 2.5 kDa. Thermal analysis of PTM showed a T_g ranging between –66 and –41 °C. PTM could be used as a plasticizer for other degradable bioplastics, sensor applications, and drug delivery. PTI, a semi-crystalline thermoset polymer, may be used for production of packaging material, disposable utensils, tableware, indoor furnishings, and more importantly, as a degradable biomaterial for biomedical applications. © 2016 Wiley Periodicals, Inc. J. Appl. Polym. Sci. **2016**, *133*, 43917.

KEYWORDS: biopolymers and renewable polymers; plasticizer; polycondensation; polyesters

Received 25 February 2016; accepted 9 May 2016

DOI: 10.1002/app.43917

INTRODUCTION

Energy savings, weight savings, and durability of polymers make them ideal substitutes for metal, paper, and glass. Since 1976, polymers have been the most used material by weight worldwide.[1] In 2013, 32.52 million tons plastic waste was generated; however, only 9.2 wt % was recycled.[2] Polymers produced from biomass-derived monomers, known as bio-based polymers, often can be biologically and/or hydrolytically degradable. Based on the environmental and economic impact of petroleum-based polymers, the need has arisen to develop biomass-based polymers that have equivalent or better properties than petroleum-based polymers. There are currently bio-based polymers on the market, but the chemical composition and subsequently thermal and mechanical properties are limited.[3–6]

Saturated and unsaturated poly-acids and poly-alcohols can be derived and/or separated from a wide range of biomass feedstock and used to develop many novel bio-based polymers with ester, anhydride, and ether linkages that are susceptible to hydrolysis and biodegradation.[7–9] Exploration of novel monomers beyond the lactic acid, glycolic acid, and 3-hydroxybutyrate acid currently used in commercial bio-based polymers is necessary to achieve a greater range of chemical and physical properties.[3–5,10] Bifunctional monomers that can be derived from biomass, such as 1,3-propanediol (PDO), malonic acid (MA), and itaconic acid (IA) are useful in the production of linear/branched copolymers that may have properties similar to those of petroleum-based polyesters.

PDO and MA are two interesting derivatives of glycerol. PDO is used in at least two commercially available polymers, Corterra PTT® from Shell Chemical Company and Sorona® from DuPont Chemical Company.[11] Research on the polymerization of PDO under a variety of polymerization conditions has been attempted with different comonomers and reaction conditions.[12–15] These prior studies with PDO provide a strong literature base from which to build a new series of polymers. MA has not been heavily studied for use in polymerizations. Dogan and Kusefoglu used MA with soy bean oil to produce a polymer with some success.[16] So, the polymerization of MA is an area of research that presents an opportunity for future research. IA is another biomonomer that could be used to produce an unsaturated polymer.[17,18] The majority of published research with IA has been in conjunction with acrylonitrile in non-polycondensation reactions.[18–20] The di-acid, unsaturated structure of IA makes it a prime candidate for polycondensation with PDO to produce unsaturated polymers. The polycondensation of PDO with MA and IA would produce novel saturated and unsaturated polyesters that have the propensity to be hydrolytically and

Additional Supporting Information may be found in the online version of this article.

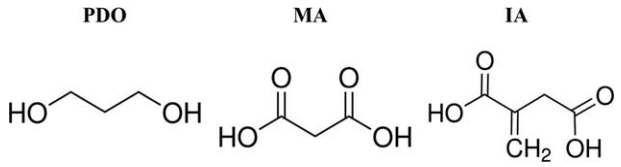

Figure 1. Chemical structure of PDO, MA, and IA monomers.

biologically degradable, so the polyesters would have the potential to be added to the portfolio of sustainable plastics available.

The properties of polymers depend on the molecular weight and molecular weight distribution. High molecular weight polymers have high strength, but also high melt viscosity and poor processability. Conversely, low molecular weight will bring about better toughness and rheological properties, but also lower rigidity. Blending polymers with low molecular weight plasticizers has been one of the most effective approaches to improve processability, flexibility, ductility, and toughness of polymers.[21,22] In our previous study, the blending of PTM with poly(lactic acid) (PLA) led to significant toughness improvement and easier processing due to lower viscosity, making PLA suitable for commercial applications.[23] In this article, we present the synthesis and characterization of a linear bio-based polymer, poly(trimethylene malonate) (PTM) and a branched, unsaturated bio-based polymer, poly(trimethylene itaconate) (PTI) with bimodal molecular weight distribution via melt polycondensation by following green chemistry principles. Green chemistry design principles state that from inception to disposal, chemicals, and chemical processes be designed to minimize hazards, maximize product utilization, use inherently less toxic chemistry, and degradation.[24] Through the careful selection of non/low toxic monomers, catalysts, and organic solvents and careful selection of reaction conditions, green chemistry principles were applied in the production of bio-based polyesters. Variable chemical structure and molecular weights were obtained and monitored as a function of reaction temperature.

EXPERIMENTAL

Materials

MA (99%, Figure 1), IA (99%, Figure 1), diethyl ether (>99%), and chloroform (98%) were purchased from VWR. PDO (98%, Figure 1), and $AlCl_3$ (98%) were purchased from Sigma-Aldrich. Tetrahydrofuran (THF, +99.9%) was purchased from Fisher Scientific. All the chemicals were used as received without further purification.

Copolymerization of 1,3-Propanediol and Malonic Acid

The melt polycondensation polymerizations were run in 100 mL round bottom flask. PDO with MA (50 g monomer) were fed in a 1:1 mole ratio with a 100:1 monomer to catalyst ($AlCl_3$) ratio. After a 5-min nitrogen purging, the flasks were immediately placed into an oil bath and allowed to react. These reactions were performed at 135, 155, and 175 °C with stirring using a magnetic stir bar and vacuum at 25 torr. After reaction, excess monomer and catalyst were removed from the reaction products by dissolving in chloroform and then poured into diethyl ether. Precipitated polymer was then filtered using Whatman (grade 40) filter paper. The filtered polymer was dried in a vacuum oven at 15 torr and 20 °C for 24 h, and then weighed.

Copolymerization of 1,3-Propanediol and Itaconic acid

In a similar way, after a 5-min nitrogen purging, the experiments were performed in a 100 mL round bottom flask (~50 g monomer) 16 h at 135, 155, and 175 °C and 25 torr with stirring. A 100:1 M/C ratio and a 1:1 acid:diol monomer ratio was maintained for all reactions. After reaction, excess monomer and catalyst ($AlCl_3$) were removed from the reaction products by dissolving in chloroform and then poured into diethyl ether. Precipitated polymer was then filtered using Whatman (grade 40) filter paper. The filtered polymer was dried in a vacuum oven at 15 torr and 20 °C for 24 h and then weighed.

Characterization

Gravimetric product yields were calculated using the limiting monomer to determine theoretical yields based on complete conversion. The recovered polymer weight was divided by the theoretical weight and then converted to percent yield. The polymer was characterized by transmission Fourier transform infrared spectroscopy (FTIR) using a Thermo Electron 6700 instrument purged with dry air. Samples were either smeared or solution cast with THF onto potassium bromide crystals. Attenuated total reflectance FTIR was also performed using a Pike VeeMax II accessory with a zinc-selenide crystal with a 60° face. A Bruker AMX-300 nuclear magnetic resonance (NMR) instrument was used to collect ^{1}H NMR spectra at 300 MHz. Samples were dissolved into deuterated chloroform and tetramethylsilane (TMS) added as an internal standard. A PHI 1600 X-ray photoelectron spectroscopy (XPS) instrument with PHI 10-360 spherical detector and achromatic Mg K_α X-ray source (300 W, 15 kV) was used to gather additional information on the chemical composition and repeat unit structure. The spectra were collected with PHI Surface Analysis Software for windows version 3.0 copyright 1994 Physical electronics Inc. and analyzed with CasaXPS version 2.2.88. The C-H peak for the carbon high resolution scan was shifted to 285 eV as a reference. Thermogravimetric analysis (TGA) was performed on a TA Instruments Q5000. Samples were analyzed from room temperature to 400 °C at 10 °C/min under nitrogen using Al_2O_3 pans. Differential scanning calorimetry (DSC) was performed using a TA Instruments Q1000 DSC with aluminum hermetic pans, purged with helium at 20 mL/min, and a heating rate of 5 °C/min from −90 to 200 °C. A Waters gel permeation chromatograph (GPC) with RI detector, 4E and 5E (polystyrene-divinylbenzene, 4.6 × 300 mm) Styragel® columns, and THF as the effluent at 0.3 mL/min was used to determine molecular weights and polydispersities. GPC was calibrated with 10-point polystyrene standards. A Rigaku SmartLab X-ray diffraction (XRD) system was used with a 2.2 kW long-fine focus X-ray tube, Bragg-Brentano para-focusing optics, and GE (220) 4-bounce incident beam monochromator with 2θ varying from 3° to 153°. In preparation for XRD, PTI samples were ground into a powder using a mortar and pestle.

RESULTS AND DISCUSSION

Synthesis of the Bio-Based Polymers

By applying green chemistry principles, the synthesis of PTM and PTI was performed by melt polycondensation. Out of the

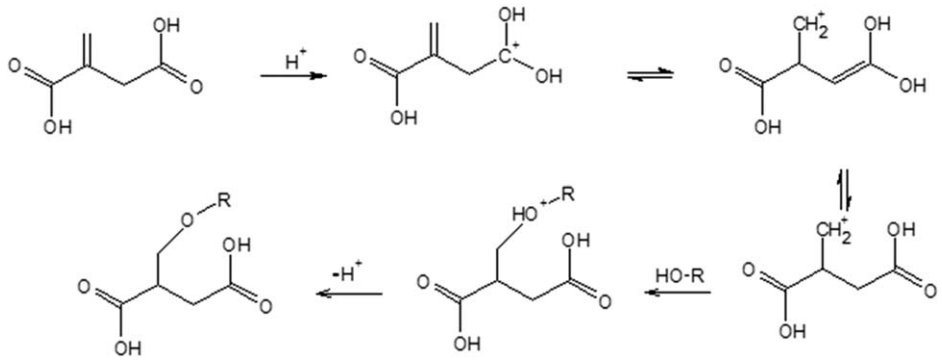

Figure 2. Mechanism for the Ordelt saturation of IA.[32]

four catalysts—aluminum chloride ($AlCl_3$), zinc chloride ($ZnCl_2$), tin (II) chloride ($SnCl_2$), and iron (III) chloride ($FeCl_3$)—studied, aluminum chloride was chosen for this study due to its higher reactivity and higher concentration of ester bonds. With the low environmental impact, aluminum chloride is relatively low cost compared to zeolites, transition metal catalysts, and rare earth catalysts. Polycondensation involving carboxylic acid and alcohol groups may follow one of four possible reversible acid-catalyzed reaction pathways.[25–28] The reactions also included oligomerization, transesterfication, Ordelt saturation, and cyclization.[29–31] Among them, Ordelt saturation (Figure 2) needs to be considered for the unsaturated monomers such as IA. Under acidic conditions, a double bond can be saturated by an alcohol group leading to polymer branching.

Gravimetric yields were determined as a function of temperature (Table I). For PTM, the 135 °C reaction product showed a considerably lower viscosity. The reaction temperature was above the melting point of MA (133 °C), and a soft, waxy solid was produced. A maximum yield of ~78% for PTM occurred at 155 °C, and then decreased with increasing temperature. At 175 °C above the decomposition point of MA (140 °C), black and brown discoloration, due to thermal degradation, are noticeable by visual inspection at approximately 2 h and increase in size with reaction time. The relatively low yields (<95%) are due to thermodynamic control of the reactions, which allow the reverse reaction to prevail in the reaction, and the entrainment of low molecular weight products in the reaction mixture. Furthermore, the reverse reaction becomes more dominant at temperatures above 155 °C, further limiting the reaction yields, because the reverse reaction is endothermic and has higher reaction rates with increasing temperature.

As shown in Table I, PTI demonstrated steady yield increased from 41% at 135 °C to a maximum of 77% at 155 °C, and then the yield was same at 175 °C. As the reaction progresses and the system increases viscosity until it becomes a gel and stirring ceases, the diffusion rate of water decreases, leading to the entrapment of water. The entrapped water reduces the driving force of the reaction to produce polymeric products and increases the reverse reaction, hydrolytic scission of the polymeric chains. The reverse reaction limits the gravimetric yields to <90%. With Ordelt saturation being temperature dependent, higher reaction temperatures produce polymers with increasing numbers of branch points.[33]

The weight-average molecular weights (M_w) and polydispersity index (PDI) were examined with GPC. In all of the GPC traces for these polymers, a bimodal molecular weight distribution with a peak above 10 kDa (HM_w) and a peak below 10 kDa (LM_w) (Supporting Information Figure S1) was noticed. The low molecular weight distribution was indicative of step growth polymerization,[29] as simultaneous polymerization, chain growth polymerization may explain the presence of the HM_w component.[29] PTM polymer was primarily a low molecular weight, waxy solid whereas PTI polymer was stiff and brittle due to branching.

Reaction temperature appears to have a significant effect on the molecular weight of PTM (Table I). The HM_w increased by ~3 kDa as temperature increased from 135 to 155 °C, and then the HM_w decreased after 165 °C as the polymer started to show visible signs of degradation, yellow to black coloration from an initially

Table I. Characterization of PTM and PTI Copolymers Polymerized at Different Conditions

Polymer	Reaction time (h)	Reaction temp (°C)	Yield (wt %)	HM_w (Da)	PDI	LM_w (Da)	T_g (°C)	T_m (°C)	T_c (°C)	$T_{5\%}$ (°C)
PTM	4	135	26	33570	1.3	1240	−65	—	—	113
	4	155	75	36580	1.3	1400	−58	—	—	201
	4	175	60	36080	1.1	2000	−42	—	—	176
PTI	16	135	41	22250	1.3	670	—	—	167	192
	16	155	77	37800	1.2	1040	—	—	163	235
	16	175	77	3870	1.8	2350	—	—	164	227

HM_w high weight—average molecular weight, LM_w low weight—average molecular weight, T_g glass transition temperature, T_m melting temperature, T_c cold crystallization peak temperature, $T_{5\%}$ temperature at 5% weight loss.

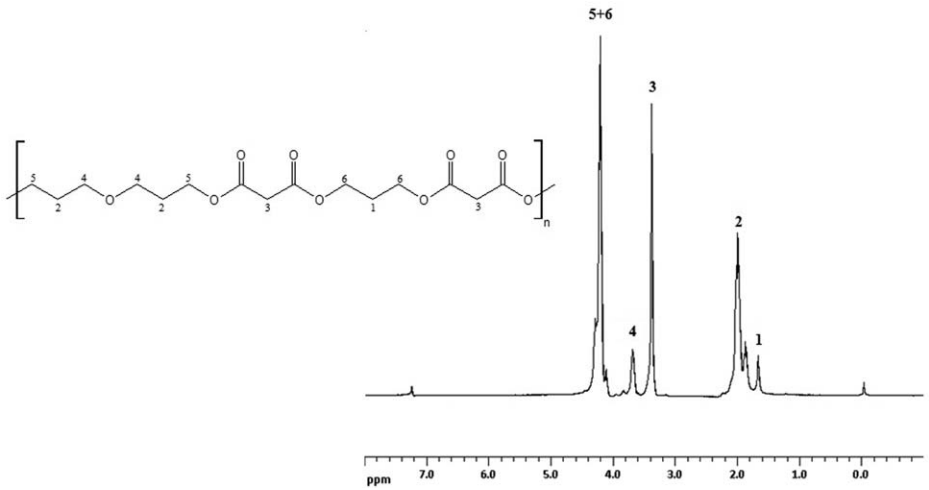

Figure 3. ^{1}H NMR spectrum of the PTM copolymer (4 h, 155 °C).

white product. The LM_w increased with reaction temperature, especially between 155 and 175 °C when degradation begins (Table I). The degradation products of HM_w are likely contributing to the apparent increase in LM_w. Furthermore, the increase in LM_w with increasing temperature is indicative of a thermodynamically controlled reaction that allows the reverse reaction to occur. The molecular weight of PTM showed a dependence on reaction temperature. Step and chain growth polymerization was expected for PTI, and Ordelt saturation was also a possibility with a methylene group on the second carbon. PTI showed a strong dependence on the reaction temperature for both HM_w and LM_w (with 1.6 and 98.4 wt %), Table I. At 175 °C, HM_w became undetectable, and the LM_w increased significantly. For both PTM and PTI bio-based polymers, maximum molecular weights of 37 and 38 kDa, respectively, were obtained at 155 °C.

Structure of the Bio-Based Polymers

^{1}H NMR analysis showed that the PTM copolymer backbone contained a mixture of alkane, ester, and ether bonds. Experimental shifts were determined although literature (Figure 3).[34–36] The model structure of PTI by the prediction of shifts can be seen in Figure 4.[34–36] NMR did indicate that branching was occurring in the polymer. The peaks for branching, 2.56 and 3.61 ppm, were relatively weak, indicating a low concentration of branch points. The specific peaks at 5.81 and 6.43 ppm are assigned to H^{12} protons from the C═C double bond of IA.

Transmission FTIR spectra were taken of all resultant polymers to determine chemical composition. FTIR spectra of monomers and the synthesized polymers are shown in Supporting Information Figure S2 and Figure 5. For PTM, a broad O—H stretch peak from approximately 3680 to 3135 cm^{-1} indicates presence of —OH groups of alcohols. Absorption peaks at 2904 and 2965 cm^{-1} correspond to C—H stretching. A strong absorption peak around 1732 cm^{-1} is attributed to carbonyl C═O stretching vibration. Peaks for C—C and C—O stretching can be seen at 1465 and 1152 cm^{-1}, respectively. The corresponding spectra of PTM and PTI were similar to their precursors, except for the

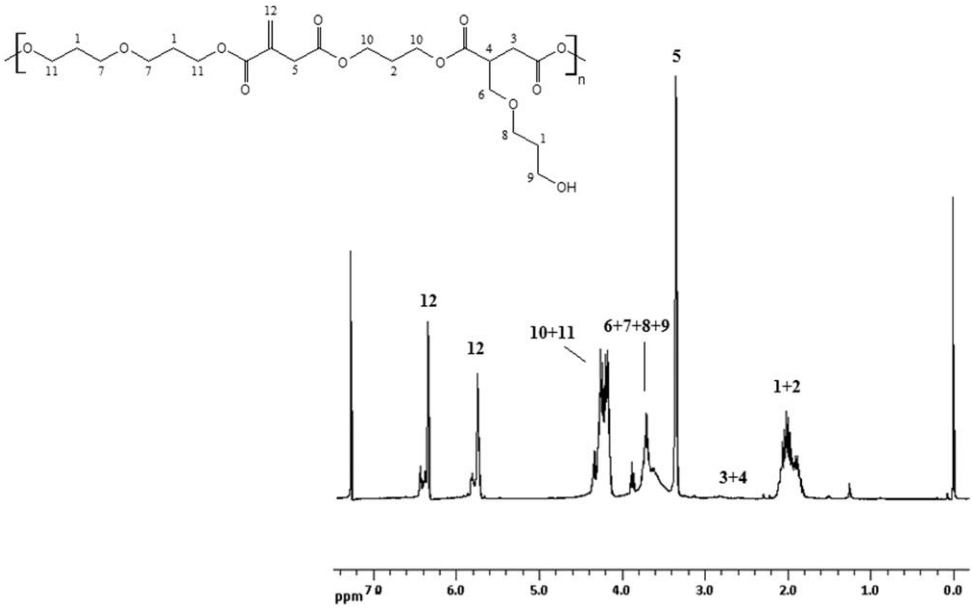

Figure 4. ^{1}H NMR spectrum of the PTI copolymer (16 h, 155 °C).

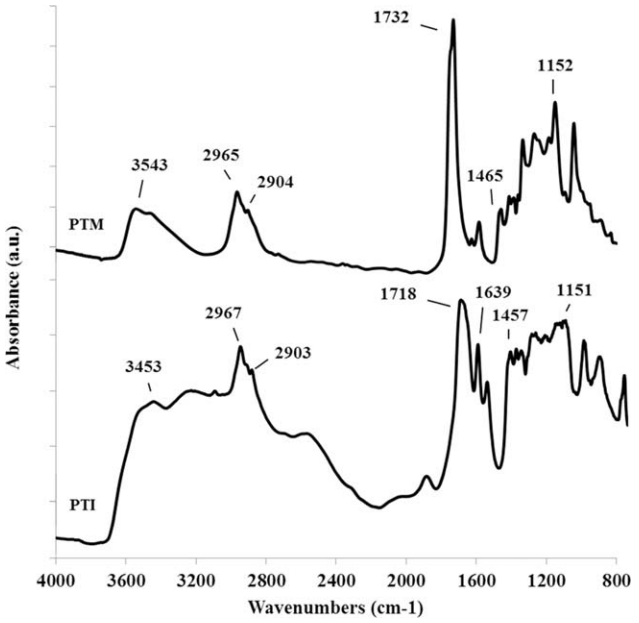

Figure 5. Representative transmission FTIR spectra of PTM and PTI made at 155 °C for 4 and 16 h, respectively.

presence of the peak at 1639 cm^{-1}, corresponding to C═C stretching in PTI.

XPS was also used to characterize PTM made at 155 °C for 4 h and PTI made at 155 °C for 16 h using aluminum chloride. The PTM and PTI survey scans (Figure 6) revealed only the presence of carbon and oxygen, and, as expected, the carbon and oxygen atomic concentrations were not in the correct ratio for PTM made of 1:1 ratio of PDO and MA units whereas they were in the correct ratio for PTI made of 1:1 ratio of PDO and IA units, Table II. For PTM, the low concentration of oxygen and high concentration of carbon indicate that PDO is preferentially being added to the polymer. Under acidic conditions, alcohols can react with other alcohols to form ether bonds.[37–39] Since

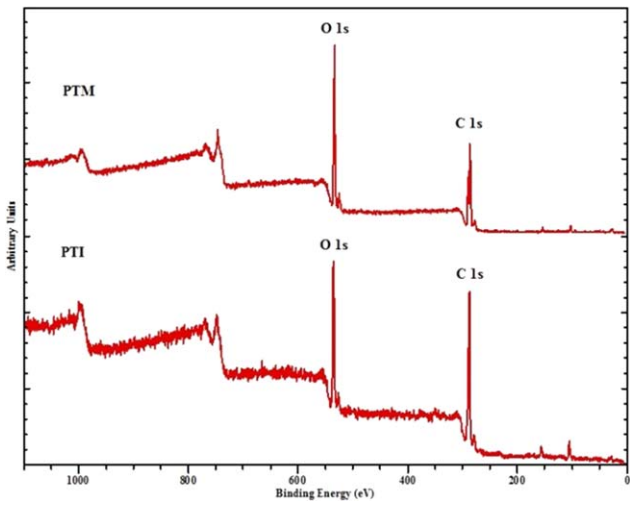

Figure 6. XPS survey spectra of PTM (155 °C, 4 h) and PTI (155 °C, 16 h). [Color figure can be viewed in the online issue, which is available at wileyonlinelibrary.com.]

Table II. Atomic Concentrations of Carbon and Oxygen in PTM and PTI, as Determined by XPS and Theoretical Concentrations

		Percent atomic concentration	
Polymer	Atom	Experimental	Theoretical
PTM	O	36.57 ± 0.72	40
	C	64.43 ± 0.72	60
PTI	O	29.99 ± 1.97	31.25
	C	70.01 ± 1.97	68.75

PDO repeat unit has a lower concentration of oxygen (25 at %) and a higher carbon content (75 at %) than MA (50 at % oxygen, 50 at % carbon), the preferential addition of PDO would cause the lower than expected oxygen content of the polymer. Conversely, for PTI, it was expected that PDO and IA would not be in the correct concentration due to branching. For PTI made at 155 °C for 16 h using aluminum chloride, branching does not appear to affect the atomic concentration of O and C. It is expected, if the extreme conditions were analyzed, that the atomic concentration of O would increase with branching.

Peak fitting of the high resolution C 1s scan for the C—H, C—O—, and C═O functional groups allowed for an accurate determination of the fractions of PDO and MA repeat units, Figure 7.[40–44] The peaks were identified as C—H at 285 eV (36.5% ± 1.2% area), C—O at 286.5 eV (37.5% ± 1.8% area), and C═O at 289.2 eV (25.6% ± 0.2% area). Determination of C—O and C═O participating in ester bonds could not be determined from the XPS results. The results show a high concentration of C—O in PTM that should have been closer to 25% area for agreement with theoretical results. The increased C—O concentration is due to a higher concentration of PDO in PTM as the survey scan results suggest.

Peak fitting of the high resolution C 1s scan for the C—H, C—O—, and C═O functional groups allowed for an accurate determination of the fractions of PDO and IA repeat units, Figure 8.[40–44] The peaks were identified as C—H at 285 eV (53.68% ± 1.56% area), C—O at 286.6 eV (28.51% ± 1.56% area), and C═O at 289.2 eV (17.81% ± 1.21% area). The theoretical calculations for C—H (54.4% area), C—O (27.27% area),

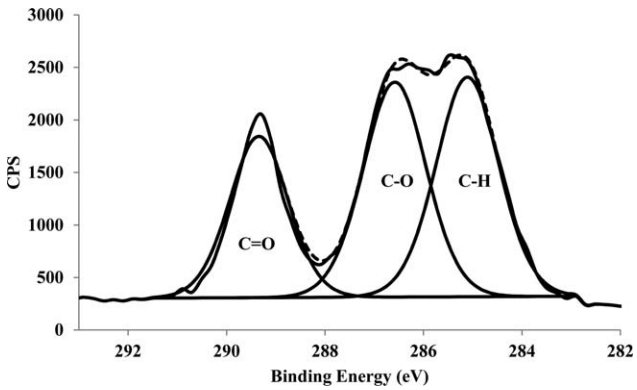

Figure 7. Peak fitting of a high resolution C 1s XPS scan for PTM (155 °C, 4 h). CPS stands for counts per second as a measure of the intensity.

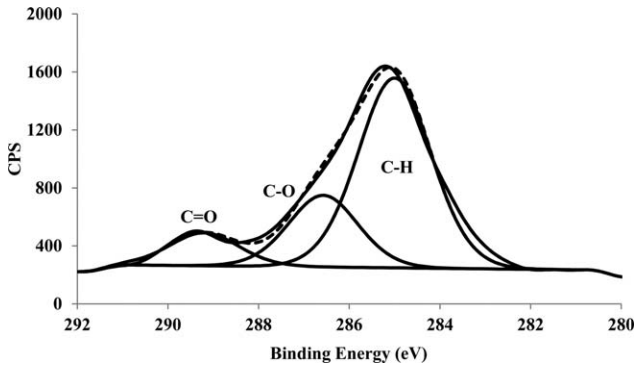

Figure 8. Peak fitting of a high resolution C 1s XPS scan for PTI (155 °C, 16 h). CPS stands for counts per second as a measure of the intensity.

and C═O at 289.2 eV (18.18%) were in close agreement with experimental results. Branching did not appear to affect functional groups concentration.

As shown in Figure 9, the XRD pattern of PTI contains a sharp crystalline peak around 20.1°. A similar result for a series of polyesters synthesized from sebacic acid, glycol, and glycerol was presented by Tang *et al.*[45] They found a single diffraction peak around 21.1°. A rounded peak would indicate the absence of crystalline material, and this is not the case for this PTI sample. However, the broadness of the peak indicates that there are crystalline, semi-crystalline, and amorphous regions in PTI. A purely crystalline material is expected to have a peak width of less than 5 degrees. PTI has a peak width of ~15 degrees indicating that the polymer does have crystalline regions.[46] The reflections at 18.8, 20.1, and 22.1° revealed crystallization of PTI (Figure 9). In a similar study, Guo *et al.* reported that the diffraction peaks around 18.9, 20.3, 21.6, and 22.4° were found in the wide-angle XRD patterns of the bio-based polyester of PDO, IA, and sebacic acid.[47] The peaks were attributed to (102), (016), (112), and (105) reflections, respectively.

Thermal Properties

TGA and DSC were performed on several representative samples from PTM and PTI samples made at 135, 155, and 175 °C (Table I). For PTM, the 135 °C sample lost 5 wt % by 113 °C, which may have been due to loss of oligomers, water, and other solvents. PTM samples made at 155 and 175 °C showed 5 wt % loss at approximately 201 °C and 176 °C, respectively, which is

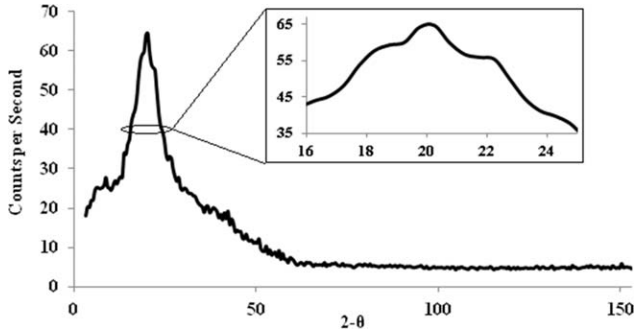

Figure 9. XRD pattern of PTI (155 °C, 16 h) from 3 to 153° at room temperature.

below the boiling point of PDO and above the boiling points of fluids that the polymer has come into contact with, including water, ether, and chloroform. In the TGA trace (Supporting Information Figure S3), an increase in the slope occurs around 210 °C, which is the boiling point of PDO, and would indicate that PDO or PDO oligomers are present in the polymer. There are no other readily discernible features above 220 °C, and by 400 °C, the sample is thermally decomposed. For PTI, the 135 °C PTI sample did not lose 5 wt % until 192 °C, which is substantially below PDO's boiling point and well above the solvents used in processing, chloroform and ether, boiling point. PTI 155 (Supporting Information Figure S4) and 175 °C samples did not have 5 wt % loss until 235 and 227 °C, respectively, Table I.

In the DSC analysis, second heating was attempted to erase the thermal history; however, the samples did not recrystallize so only the first scans (Supporting Information Figure S5 and S6) were used to determine the transition temperatures. The PTM produced at 155 °C was an amorphous copolymer with a glass transition temperature (T_g) of approximately –58 °C. DSC was performed on two other PTM samples to examine T_g as a function of reaction temperature. For the 135 °C and 175 °C PTM samples, the T_g's were measured at approximately –65 °C and –42 °C. The T_g of PTM was found to trend upwards with increasing reaction temperature. Such a low glass transition temperature of PTM may be useful for mixing/blending as an efficient plasticizer. The PTI produced at 155 °C is a semi-crystalline thermoset polymer with a cold crystallization temperature of 163 °C. Two other representative samples were also examined for PTI, samples made at 135 and 175 °C for 16 h with aluminum chloride, vacuum and stirring. For the 135 °C, there was an apparent crystallization at 167 °C, Table I, and the 175 °C PTI sample had a similar DSC curve as 155 °C PTI with a crystallization peak at 164 °C. The PTI polymer demonstrated superior thermal properties compared to PTM and may be better suited for commercial application.

CONCLUSIONS

The bio-based polyesters, PTM and PTI with bimodal molecular weight distribution, were produced from three biomonomers, PDO, MA, and IA, by following green chemistry principles. Chemical composition, yield, molecular weight, and thermal properties were found to depend on the reaction temperature. FTIR, ^{1}H NMR, and XPS showed that these polymers contained ester and ether backbone linkages. GPC data showed PTM and PTI, as produced, had a bimodal molecular weight distribution due to simultaneous step- and chain-growth polycondensation reactions. PTM and PTI could be used as renewable polymers for a wide range of commercial applications. PTM showed a T_g (–58 °C) which may make it useful in specialty applications such as sensors and biomedical applications or as a "green" additive for other polymers. Thermal analysis did not identify any crystalline portion of PTM; the combination of backbone chemistry and low molecular weight allow PTM to be susceptible to hydrolytic degradation. Research with these polymers will continue with future hydrolytic and enzymatic degradation studies.

ACKNOWLEDGMENTS

This work was partially funded through the Sustainable Energy Research Center at Mississippi State University under the Department of Energy award DE-FG3606GO86025. Financial support was also provided by MSU Bagley Fellowship. TGA and DSC were completed by Kimberly Ivey of Clemson University.

REFERENCES

1. Carole, T.; Pellegrino, J.; Paster, M. In Opportunities in the Industrial Biobased Products Industry; Finkelstein, M.; McMillan, J.; Davison, B.; Evans, B., Eds.; Humana Press: New York, **2004**; p 871.
2. Advancing Sustainable Materials Management: 2013 Fact Sheet; United States Environmental Protection Agency, **2015**.
3. Albertsson, A.-C.; Varma, I. In Aliphatic Polyesters: Synthesis, Properties and Applications; Albertsson, A.-C., Ed.; Springer: Berlin, Heidelberg, **2002**; p 1.
4. Mohanty, A. K.; Misra, M.; Hinrichsen, G. *Macromol. Mater. Eng.* **2000**, *276–277*, 1.
5. Philip, S.; Keshavarz, T.; Roy, I. *J. Chem. Technol. Biotechnol.* **2007**, *82*, 233.
6. Iwata, T. *Angew. Chem. Int. Ed* **2015**, *54*, 3210.
7. Ragauskas, A. J.; Williams, C. K.; Davison, B. H.; Britovsek, G.; Cairney, J.; Eckert, C. A.; Frederick, W. J.; Hallett, J. P.; Leak, D. J.; Liotta, C. L. *Science* **2006**, *311*, 484.
8. Dodds, D. R.; Gross, R. A. *Science* **2007**, *318*, 1250.
9. Goerz, O.; Ritter, H. *Polym. Int.* **2013**, *62*, 709.
10. Drumright, R. E.; Gruber, P. R.; Henton, D. E. *Adv. Mater.* **2000**, *12*, 1841.
11. Wemy, F. Corterra PTT—A New Polymer for the Carpet Industry; Shell Chemical Company: Rotterdam, **1999**.
12. Umare, S. S.; Chandure, A. S.; Pandey, R. A. *Polym. Degrad. Stabil.* **2007**, *92*, 464.
13. Liu, Y.; Ranucci, E.; Lindblad, M. S.; Albertsson, A. C. *J. Bioact. Compat. Polym.* **2002**, *17*, 209.
14. Ranucci, E.; Liu, Y.; Söderqvist Lindblad, M.; Albertsson, A. C. *Macromol. Rapid Commun.* **2000**, *21*, 680.
15. Witt, U.; Müller, R. J.; Augusta, J.; Widdecke, H.; Deckwer, W. D. *Macromol. Chem. Phys.* **1994**, *195*, 793.
16. Doğan, E.; Küsefoğlu, S. *J. Appl. Polym. Sci.* **2008**, *110*, 1129.
17. Willke, T.; Vorlop, K. D. *Appl. Microbiol. Biotechnol.* **2004**, *66*, 131.
18. Winkler, M.; Lacerda, T. M.; Mack, F.; Meier, M. A. R. *Macromolecules* **2015**, *48*, 1398.
19. Chen, J.; Wang, C.; Ge, H.; Bai, Y.; Wang, Y. *J. Polym. Res.* **2007**, *14*, 223.
20. Devasia, R.; Nair, C. P. R.; Sivadasan, P.; Katherine, B. K.; Ninan, K. N. *J. Appl. Polym. Sci.* **2003**, *88*, 915.
21. Pillin, I.; Montrelay, N.; Grohens, Y. *Polymer* **2006**, *47*, 4676.
22. Rasal, R. M.; Hirt, D. E. *Macromol. Mater. Eng.* **2010**, *295*, 204.
23. Eyiler, E.; Chu, I. W.; Walters, K. B. *J. Appl. Polym. Sci.* **2014**, *131*, DOI: 10.1002/app.40888.
24. Anastas, P.; Eghbali, N. *Chem. Soc. Rev.* **2010**, *39*, 301.
25. Satchell, D. P. N.; Satchell, R. S. In Mechanistic Aspects. Recent Developments Concerning Mechanisms of Acylation by Carboxylic Acid Derivatives; Patai, S., Ed.; Wiley: Chichester, UK, **2010**; p 747.
26. Smith, M.; March, J. Aliphatic Substitution: Nucleophilic and Organometallic; Wiley-Interscience: Hoboken, New Jersey, **2007**; p 425.
27. Bruckner, R. Nucleophilic Substitution Reactions on the Carboxyl Carbon; Elsevier: New York, **2002**; p 221.
28. Saunders, J. H.; Dobinson, F. In Chapter 7 The Kinetics of Polycondensation Reactions; Bamford, C. H.; Tipper, C. F. H., Eds.; Elsevier: Amsterdam, **1976**; p 473.
29. Odian, G. Principles of Polymerization; Wiley: New York, **1991**; p 41.
30. Kricheldorf, H. R. *Macromol. Rapid Commun.* **2007**, *28*, 1839.
31. Salmi, T.; Paatero, E.; Nyholm, P. *Chem. Eng. Process.* **2004**, *43*, 1487.
32. Fradet, A.; Marechal, E. *Die Makromol. Chem.* **1982**, *183*, 319.
33. Fradet, A.; Maréchal, E. Kinetics and Mechanisms of Polyesterifications; Springer: Berlin, Heidelberg, **1982**; p 51.
34. Agrawal, J. P.; Montheard, J. P. *J. Macromol. Sci. Part A* **1993**, *30*, 59.
35. Qian, H.; Mathiowitz, E. *J. Polym. Sci., Part A: Polym. Chem.* **2007**, *45*, 5899.
36. Pretsch, E.; Buhlmann, P.; Affolter, C. Tables of Spectral Data; Springer: Berlin, **2000**; p 161.
37. Dellerba, R.; Martuscelli, E.; Musto, P.; Ragosta, G.; Leonardi, M. *Polym. Networks Blends* **1997**, *7*, 1.
38. Silverstein, R.; Bassler, G. C.; Morrill, T. C. Spectrometric Identification of Organic Compounds; Wiley: Hoboken, NJ, **1991**; p 102.
39. Dean, J. A. Lange's Handbook of Chemistry; McGraw-Hill: New York, **1992**; p 7.42.
40. Sabbatini, L.; Zambonin, P. G. *J. Electron. Spectrosc. Relat. Phenomena* **1996**, *81*, 285.
41. Louette, P.; Bodino, F.; Pireaux, J. *J. Surf. Sci. Spectra* **2005**, *12*, 38.
42. Louette, P.; Bodino, F.; Pireaux, J. *J. Surf. Sci. Spectra* **2005**, *12*, 69.
43. Cossement, D.; Gouttebaron, R.; Cornet, V.; Viville, P.; Hecq, M.; Lazzaroni, R. *Appl. Surf. Sci.* **2006**, *252*, 6636.
44. Nansé, G.; Papirer, E.; Fioux, P.; Moguet, F.; Tressaud, A. *Carbon* **1997**, *35*, 175.
45. Tang, J.; Zhang, Z.; Song, Z.; Chen, L.; Hou, X.; Yao, K. *Eur. Polym. J.* **2006**, *42*, 3360.
46. Roe, R.-J. Methods of X-Ray and Neutron Scattering in Polymer Science; Oxford University Press: New York, **2000**; p 130.
47. Guo, B.; Chen, Y.; Lei, Y.; Zhang, L.; Zhou, W. Y.; Rabie, A. B. M.; Zhao, J. *Biomacromolecules* **2011**, *12*, 1312.